Multinuclear NMR Study of the Structure of the Fv Fragment of Anti-Dansyl Mouse IgG2a Antibody†

Hideo Takahashi,‡ Asano Odaka,‡ Shunro Kawaminami,§ Chigusa Matsunaga,‡ Koichi Kato,‡ Ichio Shimada,‡ and Yoji Arata*,‡

Faculty of Pharmaceutical Sciences, University of Tokyo, Hongo, Tokyo 113, Japan, and Biological Science Laboratories, Kao Corporation, Akabane Ichikaimachi, Haga, Tochigi 321-34, Japan

Received February 12, 1991; Revised Manuscript Received April 11, 1991

ABSTRACT: A multinuclear NMR study is reported of Fv, which is a minimum antigen-binding unit of immunoglobulin. Fv has been prepared by clostripain digestion of a mouse anti-dansyl IgG2a monoclonal antibody that lacks the entire C_H1 domain [Takahashi, H., Igarashi, T., Shimada, I., & Arata, Y. (1991) *Biochemistry 30*, 2840–2847]. A variety of Fv analogues labeled with ^2H in the aromatic rings and with ^{13}C and/or ^{15}N in the peptide bonds have been prepared and used for multinuclear NMR analyses of Fv in the absence and presence of ε-dansyl-L-lysine (DNS-Lys). It has been shown that ^1H–^{15}N shift correlation spectra of Fv sensitively reflect the antigen binding and can be used along with ^1H and ^{13}C spectral data for the structural analyses of antigen–antibody interactions. Hydrogen–deuterium exchange of the amide protons has been followed in the absence and presence of DNS-Lys by using the ^1H–^{15}N shift correlation spectra. Use of the β-shift observed for the carbonyl carbon resonances has also been helpful in following the hydrogen–deuterium exchange. On the basis of the NMR data obtained, the static and dynamic structure of the Fv fragment in the absence and presence of DNS-Lys has been discussed.

Immunoglobulin G (IgG)[1] consists of two identical heavy chains and two identical light chains. The heavy chains are composed of four homology units, V_H, C_H1, C_H2, and C_H3, whereas the light chains are divided into two homology units, V_L and C_L. It is known that the antigen-binding site is constructed by six CDR loops, three each from the V_H and V_L domains. The six CDR loops are highly variable both in length and in the amino acid sequences, and the degree of contribution from each of these CDR loops to antigen binding varies for different antibodies. The antigen-binding site is constructed on a *β-barrel* that is essentially common to all antibody molecules and forms a scaffold supporting the CDR loops (Lesk & Chothia, 1982).

The Fv fragment, which is a heterodimer of V_H and V_L domains, is a minimum antigen-binding unit with a molecular weight of 25 000 (Inbar et al., 1972). Although Fv fragment is attractive for a detailed structural analysis of the mechanism of antigen recognition, preparation of a large amount of Fv by proteolytic cleavage of the intact IgG has been attempted with little success (Inbar et al., 1972; Hochman et al., 1973; Sharon & Givol, 1976). In a previous paper (Takahashi et al., 1991) we have shown that the Fv fragment can be prepared in high yield by limited proteolysis with clostripain of a short-chain mouse IgG2a anti-dansyl monoclonal antibody in which the entire C_H1 domain is deleted (Igarashi et al., 1990). Fv fragments have recently been expressed by using *Escherichia coli* (Skerra & Plückthun, 1988; Huston et al., 1988; Ward et al., 1989; Boulot et al., 1990) as well as myeloma cells (Riechmann et al., 1988). Wright et al. (1990) have outlined a general strategy for spectral assignments using an anti-lysozyme Fv fragment expressed by myeloma cells.

Selective isotope labeling was first used by Jardetzky and co-workers in order to obtain information about the protein structure in solution (Markley et al., 1968). Multinuclear NMR techniques are now in extensive use for the determination of solution structures of proteins of $M_r \lesssim 20000$ (Markley, 1989). In the previous paper, we reported a NOESY study of an Fv analogue, in which all aromatic protons except for His C2′-H and Tyr C3′,5′-H had been selectively deuterated (Takahashi et al., 1991). On the basis of the NOESY data obtained in the absence and presence of DNS-Lys, all the ring proton resonances for the dansyl group that is bound to the Fv fragment have been assigned. It has been concluded that two Tyr residues along with one of the amide groups are directly involved in the antigen binding.

We have also reported a ^{13}C NMR study that makes use of IgGs and their functional fragments labeled with ^{13}C at the carbonyl carbon. It has already been demonstrated that even with the intact antibody with a molecular weight of 150K the carbonyl carbon resonances can be observed separately and site-specific assignments of each of the resonances are possible (Kato et al., 1989a, 1991a,b).

In the present paper we report a multinuclear NMR approach to the structure of Fv fragment. A variety of Fv fragments singly and doubly labeled with ^2H, ^{13}C, and ^{15}N

† This research was supported in part by special coordination funds for promoting science and technology from the Science and Technology Agency and by grants from the Ministry of Education, Science, and Culture of Japan (62870089 and 63430022).

* To whom correspondence should be addressed.
‡ University of Tokyo.
§ Kao Corporation.

[1] Abbreviations: CDR, complementarity-determining region; CDR1(H), CDR2(H), CDR3(H), CDR in the V_H domain; CDR1(L), CDR2(L), CDR3(L), CDR in the V_L domain; DNS-Lys, ε-dansyl-L-lysine; HPLC, high-performance liquid chromatography; FR, framework region; FR1(H), FR2(H), FR3(H), FR in the V_H domain; FR1(L), FR2(L), FR3(L), FR in the V_L domain; Fv, antigen-binding fragment composed of V_H and V_L; HMQC, heteronuclear multiple-quantum correlation; HOHAHA, homonuclear Hartmann–Hahn spectroscopy; IgG, immunoglobulin G; NMR, nuclear magnetic resonance; NOESY, two-dimensional NOE correlated spectroscopy; V_H, the variable domain of the heavy chain; V_L, the variable domain of the light chain.

0006-2960/91/0430-6611$02.50/0

were prepared. Spectral assignments will be made as described previously (Kato et al., 1989a, 1991a,b). Carbonyl carbon ^{13}C NMR spectra and ^{1}H–^{15}N shift correlation spectra will be used to discuss antigen–antibody interactions. The rate of hydrogen–deuterium exchange of the amide protons of Fv is followed in the absence and presence of DNS-Lys. On the basis of the NMR data obtained, the static and dynamic structure of the Fv fragment will be discussed.

Materials and Methods

Materials. L-[1-^{13}C]Tyr was prepared by an enzymatic coupling reaction of phenol and sodium [1-^{13}C]pyruvate in the presence of CH_3COONH_4 by using β-tyrosinase (Nagasawa et al., 1981). L-[1-^{13}C, ^{15}N]Tyr was prepared by a similar reaction, in which CH_3COONH_4 was replaced by [^{15}N]NH_4Cl. L-[^{15}N]Tyr was purchased from Isocommerz GmbH, Germany. [1-^{13}C]Cystine was a gift of Dr. N. Sugita. All other ^{13}C- and ^{15}N-labeled amino acids were purchased from ICON Services Inc., USA. The isotope enrichment is 95% or higher for each of these amino acids. Clostripain was obtained from Sigma Chemical Co. All other chemicals were of reagent grade and used without further purification.

Preparation of Stable-Isotope-Labeled Analogues of the Fv Fragment of the Anti-Dansyl Mouse IgG2a Antibody. The mouse hybridoma cell line, 1B10.7, which produces the short-chain mouse IgG2a anti-dansyl monoclonal antibody (Dangl et al., 1982; Igarashi et al., 1990), was adapted to a serum-free medium (Nissui NYSF 404) and then grown in the medium containing stable-isotope-labeled amino acid(s) (Kato et al., 1989a,b, 1991). In incorporating ^{15}N-labeled amino acids, β-chloro-L-alanine was added to the medium to suppress the isotope dilution (Kato et al., 1991a). All ^{2}H, ^{13}C, and ^{15}N analogues of Fv were prepared by clostripain digestion of the short-chain antibody as described previously (Takahashi et al., 1991).

The V_H and V_L chains were isolated from Fv that had specifically been labeled. The labeled V_H and V_L chains were recombined respectively with V_L and V_H chains isolated from the unlabeled preparations of the corresponding Fv fragment. Recombination of the V_H chain and the V_L chain was performed as described previously for the intact IgGs (Kato et al., 1991a; Takahashi et al., 1991).

Iodination Reaction of Fv. A total of 300 nmol of Fv was dissolved in 15.3 mL of 100 mM phosphate buffer, pH 8.0, containing 200 mM NaCl. An aqueous solution of I_2 (10 mM) containing 100 mM KI was gradually added to the Fv solution of 0 °C until the molar ratio of I_2:Fv became 0.5. The reaction mixture was diluted with a 5 mM phosphate buffer, pH 5.0, containing 200 mM NaCl in D_2O and concentrated by ultrafiltration. For NMR measurements, the buffer of the solution thus obtained was replaced with a 5 mM phosphate buffer, pH 7.4, containing 200 mM NaCl in D_2O.

NMR Measurements. Most of the NMR spectra were acquired on a Bruker AM 400 spectrometer equipped with an ASPECT 3000 computer. Additional hardwares on this instrument included a *reverse* broadband probe and a 5W BFX-5 X-nuclear decoupler.

^{13}C NMR spectra were recorded at 100 MHz by using a Waltz 16 composite pulse decoupling sequence. The free induction decay was recorded with 32K data points and a spectral width of 24000 Hz. For resolution enhancement, the free induction decay was multiplied by a Gaussian window function prior to Fourier transformation.

Two-dimensional ^{1}H–^{15}N shift correlation (Bodenhausen & Rubern, 1980; Norwood et al., 1989) and HMQC–HOHAHA (Gronenborn et al., 1989) spectra were recorded with spectral widths of 5600 Hz for ^{1}H and 800 Hz for ^{15}N. A total of 2K data points were used in the t_2 dimension, and 160–1024 transients were acquired for each of 200 t_1 points. Mixing time was set to 17.5 ms for the measurement of HMQC–HOHAHA spectra. Two-dimensional spectra were obtained in the pure absorption mode with time-proportional phase incrementation (TPPI) (Marion & Wüthrich, 1983). Prior to 2D Fourier transformation, the acquired data were multiplied by a Gauss function in t_2 and by a shifted sine square function in t_1 and were zero-filled to yield a matrix 1024 (F_2) × 128 (F_1) of the real data points. The $^{3}J_{HN\alpha}$ coupling constants were determined from the HMQC spectra (Mueller, 1979; Redfield, 1983; Bax et al., 1983; Kay & Bax, 1990) measured with spectral widths of 7000 Hz for ^{1}H and 1250 Hz for ^{15}N on a GE Omega 500 spectrometer in the phase-sensitive mode (States et al., 1982). A total of 256 blocks were acquired with data points of 2K in the t_2 dimension. The acquired data were multiplied by an exponential function in t_2 and by a sine-bell function in t_1 and were zero-filled to yield a matrix 1024 (F_2) × 512 (F_1) of the real data points. The solvent resonance was suppressed by selective irradiation during the preparation period of 1.2 s.

For ^{13}C NMR measurements, protein solutions were concentrated by ultrafiltration to a final volume of 2 mL in 5 mM phosphate buffer, pH 7.4, containing 0.2 M NaCl. The samples were prepared in D_2O or in H_2O that contains 10% D_2O. ^{1}H–^{15}N shift correlation spectra were measured by using protein solutions concentrated by ultrafiltration to 0.4 mL in 5 mM phosphate buffer, pH 5.0, containing 0.2 M NaCl.

Hydrogen–deuterium exchange of the amide proton was followed by making use of the isotope shift observed through ^{13}C resonances of the carbonyl carbon (Kainosho & Tsuji, 1982) or by observing the intensity of the cross-peaks in the ^{1}H–^{15}N shift correlation spectra. Protein solutions used for measurements of hydrogen–deuterium exchange were prepared as described above at 4 °C, except that the buffer was prepared with 99.9% D_2O. The probe temperature was 30 °C throughout the experiment.

Results

For brevity, Fv analogues labeled with ^{13}C at the carbonyl carbon of Tyr, Trp, His, and Cys will be designated by use of the one-letter abbreviation for the amino acid as [Y]Fv, [W]Fv, [H]Fv, and [C]Fv, respectively. Fv labeled with [^{15}N]Tyr will be referred to as [^{15}N]Fv. An Fv analogue selectively labeled with Phe-*2′,3′,4′,5′,6′-d*$_5$, Trp-*2′,4′,5′,6′,7′-d*$_5$, His-*4′-d*$_1$, and Tyr-*2′,6′-d*$_2$ will be designated as [^{2}H]Fv.

^{1}H NMR Spectra of [^{2}H]Fv. Figure 1 compares the ^{1}H NMR spectra of [^{2}H]Fv observed before and after the iodination reaction. As Figure 1 shows, iodination of the Fv analogue resulted in a significant loss in intensity of resonances I and J. No other Tyr resonances showed any significant change in intensity upon iodination. In order to locate the modified two Tyr residues in the amino acid sequences, modified and unmodified Fv fragments were subjected to HPLC analyses after treatment of reduction and alkylation and lysyl endopeptidase digestion. HPLC profiles obtained are given in Figure 2. It was confirmed by peptide sequencing analysis that the peak indicated by the arrow in the profile for iodinated Fv corresponds to the peptide fragment Arg-Arg-Val-Tyr-Leu-Gln-Met-Asn-Thr-Leu-Arg-Ala-Glu-Asp-Thr-Gly-Ile-Tyr-Tyr-Cys-Thr-Gly-Ile-Tyr-Tyr*-His-Tyr*-Pro-Trp-Phe-Ala-Tyr-Trp, which contains two iodinated Tyr residues (Tyr-97H and Tyr-99H, shown by the asterisks).[2]

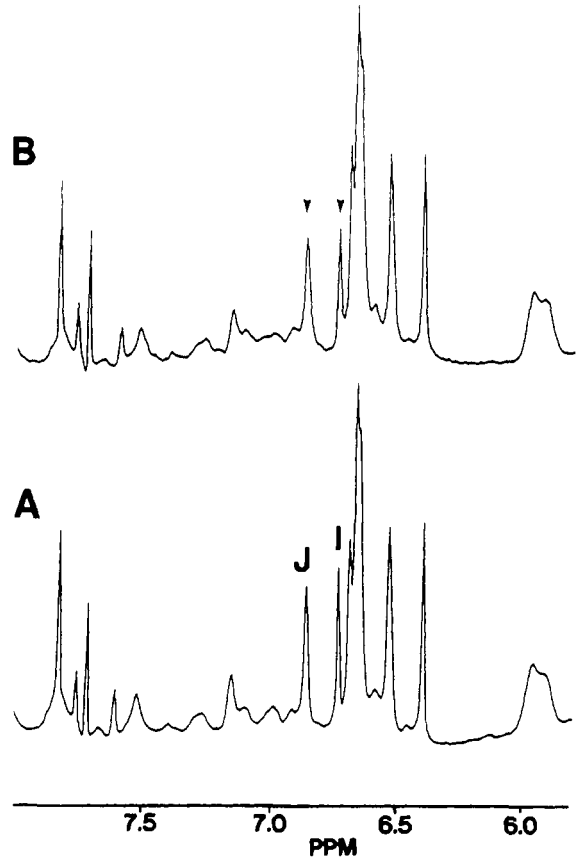

FIGURE 1: Effects of chemical modification of Fv; 400-MHz ^1H NMR spectra of [^2H]Fv (A) unmodified and (B) modified with iodinate. Resonances I and J are significantly affected by iodination (B). Measurements were made at 30 °C, pH 7.4.

Table I: Distribution of X-Tyr Dipeptides in the Anti-Dansyl Fv Fragment

Tyr[a]	location	X
58H	CDR2(H)	Thr-57H
59H	CDR2(H)	Tyr-58H
79H	FR3(H)	Val-78H
90H	FR3(H)	Ile-89H
91H	FR3(H)	Tyr-90H
96H	CDR3(H)	Ile-95H
97H	CDR3(H)	Tyr-96H
99H	CDR3(H)	His-98H
104H	CDR3(H)	Ala-103H
32L	CDR1(L)	Thr-31L
36L	FR2(L)	Trp-35L
49L	FR2(L)	Ile-48L
86L	FR3(L)	Val-85L

[a] Residues in the heavy and light chains are differentiated by H and L, respectively.

This result clearly indicates that resonances I and J are due to Tyr-97H and Tyr-99H, respectively, or vice versa. We have already shown on the basis of NOESY data that in the Fv–DNS-Lys complex Tyr J is in close contact with ring protons 2 and 3 of the dansyl group (Takahashi et al., 1991).

^1H–^{15}N Shift Correlation Spectra of [^{15}N]Fv. The Fv fragment contains 13 Tyr residues, nine from V_H and four from

[2] Sequence data of the V_H region of the antibody used in the present work has been given by J. L. Dangl (1986). Sequence data of the V_L region were kindly provided by Professor L. A. Herzenberg, Stanford University, and Dr. V. T. Oi, Becton Dickinson Immunocytometry Systems, prior to publication. The convention of Kabat et al. (1987) has been followed for the numbering of the V_H and V_L regions of the antibody.

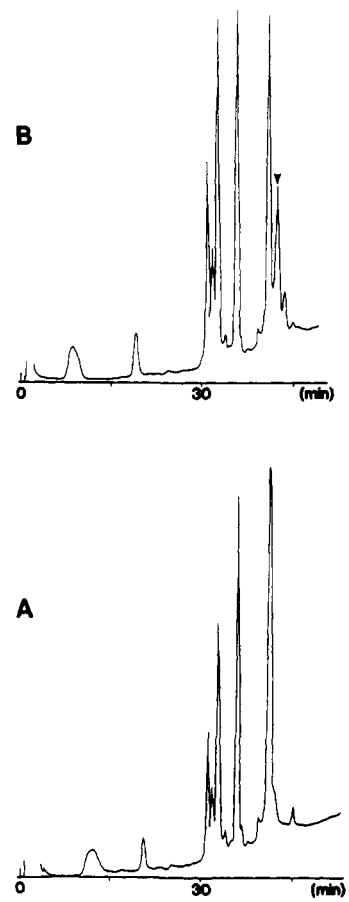

FIGURE 2: Separation on a Toso TSK gel phenyl 5PW-RP HPLC column of the products obtained by treatment of reduction and alkylation followed by lysyl endopeptidase digestion of the intact Fv (A) and the iodinated Fv (B). The products were eluted at 1 mL/min with a linear gradient of 0–60% acetonitrile in 0.1% trifluoroacetic acid over 60 min. Absorbance was detected at 230 nm. The peak indicated by the arrow for the iodinated Fv was subjected to a protein sequencing analysis (see text).

V_L (see Table I). As Figure 3A shows, except peaks j and k, which partially overlap with each other, all other peaks can be separately observed in the ^1H–^{15}N shift correlation spectrum. Some of the cross-peaks are weak in intensity, presumably due to the loss of phase information during the four $1/(4J)$ delays used in the pulse sequence. This is most likely caused by rapid chemical exchange, resulting in saturation transfer of the magnetization between the amide and water protons.

(i) Spectral Assignment. First, each of the Tyr peaks was assigned to either V_H and V_L. The ^{15}N-labeled V_H and V_L were separated from [^{15}N]Fv by treatment with guanidinium chloride, and then recombined, respectively, with unlabeled V_L and V_H. Two kinds of Fv fragments, in which either the heavy chain or the light chain is selectively labeled with [^{15}N]Tyr, were obtained by recombination of ^{15}N-labeled $V_H(V_L)$ and unlabeled $V_L(V_H)$. Figure 3B shows the ^1H–^{15}N shift correlation spectrum of a recombined Fv that is labeled with [^{15}N]Tyr only in the light chain. Comparison of parts A and B of Figure 3 clearly indicates that peaks b, d, f, and m are due to V_L. Thus, we were able to make *chain-specific* assignments of all the cross-peaks to either V_H or V_L.

Site-specific assignments of the ^1H–^{15}N cross-peaks were performed by using a double-labeling method (Kainosho & Tsuji, 1982). For this purpose, Fv was doubly labeled with [^{15}N]Tyr and [1-^{13}C]X, where X is one of amino acid residues given in Table I. ^1H–^{15}N cross-peaks originating from the

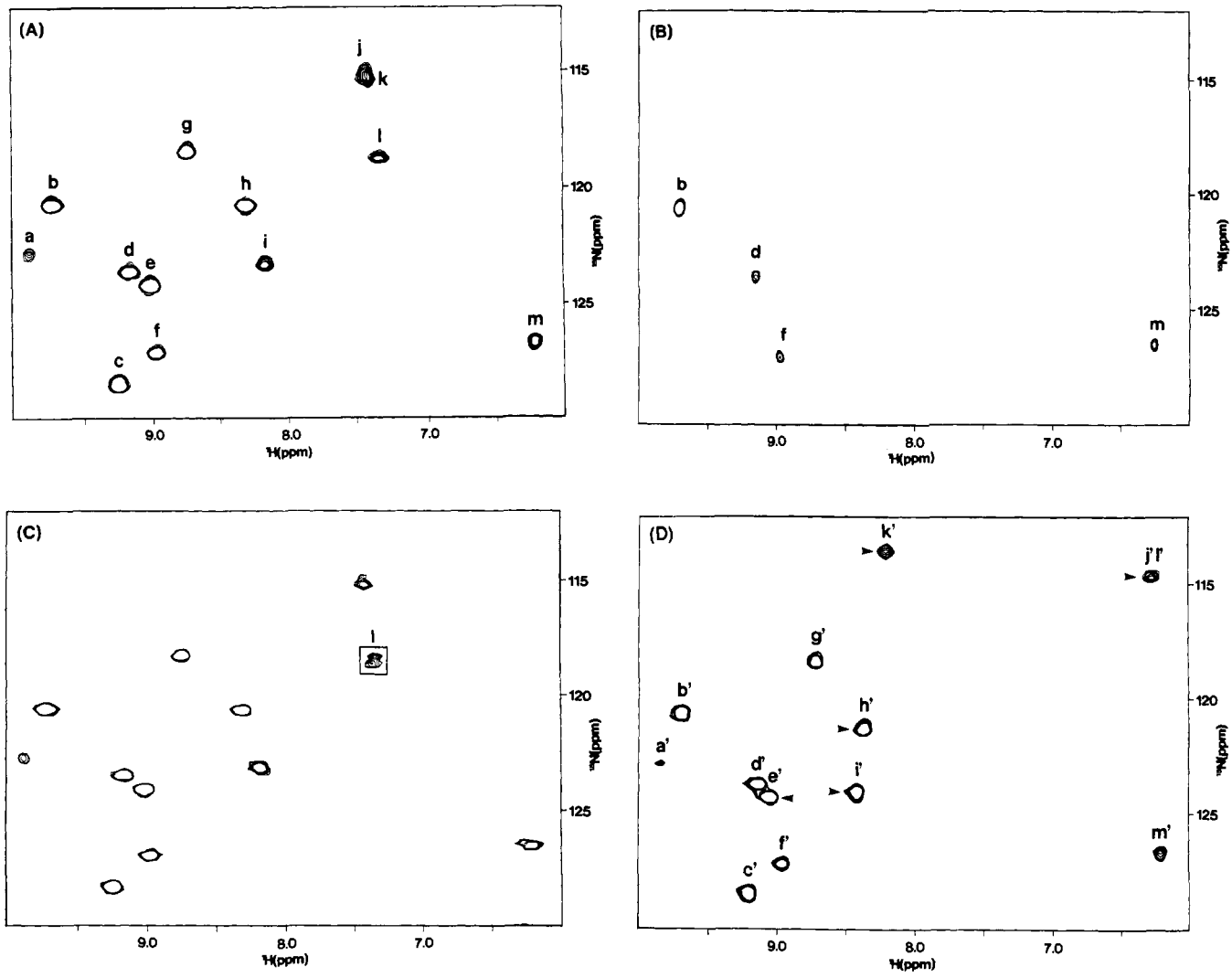

FIGURE 3: ^1H–^{15}N shift correlation spectra of [^{15}N]Fv in the absence (A, B, and C) and presence (D) of DNS-Lys. Details of the NMR measurements are described under Materials and Methods. The Fv fragment was dissolved at a concentration of 1.5 mM in 5 mM phosphate buffer containing 200 mM NaCl in H_2O, pH 5.0. The probe temperature was 30 °C. (A) [^{15}N]Fv. (B) Fv labeled with [^{15}N]Tyr only in the light chain. Samples were prepared as described under Materials and Methods. (C) Fv doubly labeled with [^{15}N]Tyr and [1-^{13}C]His. The cross-peak marked by the square is split and, therefore, assigned to Tyr-99H (see Table I). (D) [^{15}N]Fv in the presence of DNS-Lys. The Fv:DNS-Lys molar ratio was 1:1. Cross-peaks indicated by the arrows showed a significant shift upon addition of DNS-Lys. No other peaks are affected at all upon addition of DNS-Lys.

[1-^{13}C]X-[^{15}N]Tyr dipeptide can unambiguously be identified in the ^1H–^{15}N shift correlation spectrum by observing splitting due to the ^{15}N–^{13}C spin coupling ($^1J_{CN} \sim 15$ Hz). As an example, the ^1H–^{15}N shift correlation spectrum of an Fv analogue that is doubly labeled with [1-^{13}C]His and [^{15}N]Tyr is given in Figure 3C. As Table I shows, Tyr-99H is the only one Tyr that is preceded by His. Thus, cross-peak 1 can unambiguously be assigned to Tyr-99H. In a similar way, cross-peaks b and k were assigned to Tyr-36L and Tyr-104H, respectively.

In the ^1H–^{15}N shift correlation spectrum of an Fv analogue doubly labeled with [1-^{13}C]Val and [^{15}N]Tyr, cross-peaks e and f show the $^1J_{CN}$ coupling along the nitrogen chemical shift axis. The *chain-specific* assignment described above has shown that cross-peaks e and f originate from V_H and V_L, respectively. Thus, inspection of Table I led to unambiguous assignments of peaks e and f to Tyr-79H and Tyr-86L, respectively. In a similar way, cross-peaks h and m were assigned to Tyr-58H and Tyr-32L, respectively.

As Table I shows, both Ile-Tyr and Tyr-Tyr dipeptides appear three times in the amino acid sequences of the Fv fragment used in the present experiment. ^1H–^{15}N cross-peaks originating from Tyr-49L, Tyr-90H and Tyr-96H, all of which are preceded by Ile, can unambiguously be identified by using Fv doubly labeled with [1-^{13}C]Ile and [^{15}N]Tyr. The ^1H–^{15}N shift correlation spectrum for this analogue indicates that the three cross-peaks c, d, and j are split by $^1J_{CN}$ coupling (data not shown). It should be noted that the V_L contains only one Ile-Tyr dipeptide. The recombination experiment described above indicates that peak d originates from the V_L. Therefore, peak d can unambiguously be assigned to Tyr-49L. Site-specific assignments of resonances c and j were not possible by the double-labeling experiment alone. For the identification of resonances originating from Tyr-59H, Tyr-91H, and Tyr-97H, all of which are preceded by another Tyr, an Fv analogue labeled with [1-^{13}C, ^{15}N]Tyr was prepared. Peaks a, g, and i were split by $^1J_{CN}$ coupling and therefore are identified as originating from these three Tyr residues (data not shown). However, site-specific assignments for these three resonances are not possible by the double-labeling method alone. Comparisons of the ^1H–^{15}N shift correlation spectra observed in the absence and presence of DNS-Lys were helpful in assigning some of these Tyr resonances originating from the Ile-Tyr and Tyr-Tyr dipeptides (vide infra). The results of the spectral

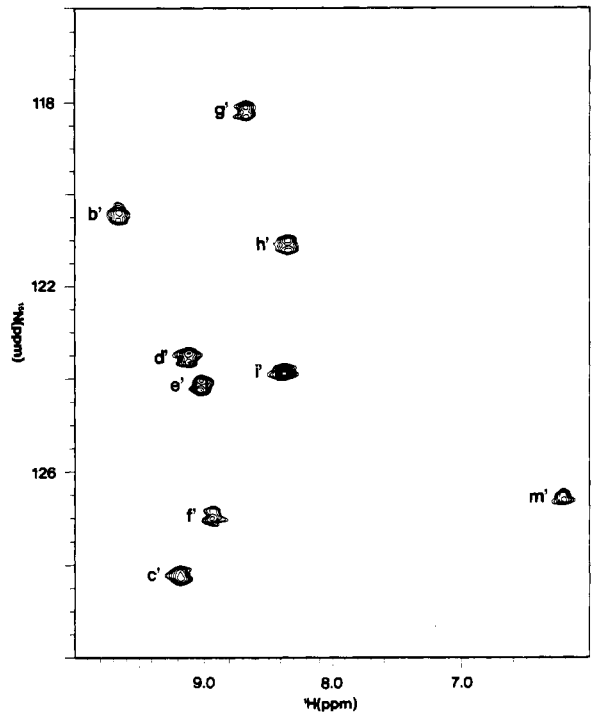

FIGURE 4: ^1H–^{15}N HMQC spectrum of [^{15}N]Fv in H_2O in the presence of DNS-Lys; 30 °C, pH 5.0. Resonances b′, d′, e′, f′, g′, and h′ show splitting due to $^3J_{HN\alpha}$. It was not possible to observe peaks a′, j′, k′, and l′ due to a strong window function applied in the t_1 dimension. Details of the spectral measurements are described under Materials and Methods.

assignments are summarized in Table II.

(*ii*) *Effects of DNS-Lys on the ^1H–^{15}N Shift Correlation Spectra of [^{15}N]Fv.* Figure 3D shows the ^1H–^{15}N shift correlation spectrum of [^{15}N]Fv observed in the presence of DNS-Lys. Upon antigen binding, peaks i, j, k, and l showed a large change in chemical shift in both the ^1H and ^{15}N dimensions, giving peaks i′, j′, k′, and l′, respectively. We have confirmed the correspondence of each pair of these peaks observed in the absence and presence of DNS-Lys by using doubly labeled Fv analogues.

Peaks l and k have already been assigned to Tyr-99H and Tyr-104H, respectively. This means that peaks l′ and k′ are due to the Tyr-99H and Tyr-104H of Fv that binds DNS-Lys, respectively. Peak j′, which is superimposed on peak l′ in Figure 3D, can separately be observed by using Fv incubated in D_2O. This is because there is a large difference in the rate of hydrogen–deuterium exchange for peaks j′ and l′ (vide infra). Peak l′, which is due to Tyr-99H, quickly disappeared on incubation in D_2O, whereas peak j′ was resistant to hydrogen–deuterium exchange under the present condition. This has been confirmed by using two kinds of [^{15}N]Fv analogues that are doubly labeled with [1-^{13}C]Ile and [1-^{13}C]His.

Table II: Assignment of Cross-Peaks Observed in the ^1H–^{15}H Shift Correlation Spectrum of [^{15}N]Fv

peak	assignment	peak	assignment
a	Tyr-91H or Tyr-59H[a]	h	Tyr-58H
b	Tyr-36L	i	Tyr-97H
c	Tyr-90H	j	Tyr-96H
d	Tyr-49L	k	Tyr-104H
e	Tyr-79H	l	Tyr-99H
f	Tyr-86L	m	Tyr-32L
g	Tyr-59H or Tyr-91H[a]		

[a] See text.

As described above, peaks i and j originate from the Ile-Tyr and Tyr-Tyr dipeptides, respectively, and therefore cannot be assigned by the double-labeling method. The present observation that peaks i and j are affected to a large extent in the presence of DNS-Lys will be used for the assignments of these two peaks (vide infra).

HMQC Spectra of [^{15}N]Fv. In order to determine the $^3J_{HN\alpha}$-coupling constant for the Tyr residues of [^{15}N]Fv in the presence of DNS-Lys, an HMQC spectrum was observed. A comparison of the ^1H–^{15}N shift correlation spectrum shown in Figure 3D and the HMQC data given in Figure 4 indicates that resonances b′, d′, e′, f′, g′, and h′ possess $^3J_{HN\alpha}$-coupling constants that are in the range of 9–11 Hz. By constrast, $^3J_{HN\alpha}$ is undetectably small for resonances c′, i′, and m′.

Figure 5 shows an HMQC–HOHAHA spectrum of [^{15}N]Fv measured in the presence of DNS-Lys. This result indicates that peaks a′, b′, d′, e′, f′, j′/l′, and m′ show the ^{15}N–$C_\alpha H$ connectivity. Among these peaks, the α-proton chemical shifts for peaks a′, b′, d′, e′, and f′ are in the range of 5.0–5.8 ppm. Peaks b′, d′, e′, and f′ have already been assigned to Tyr-36L, Tyr-49L, Tyr-79H, and Tyr-86L, respectively (see Table II).

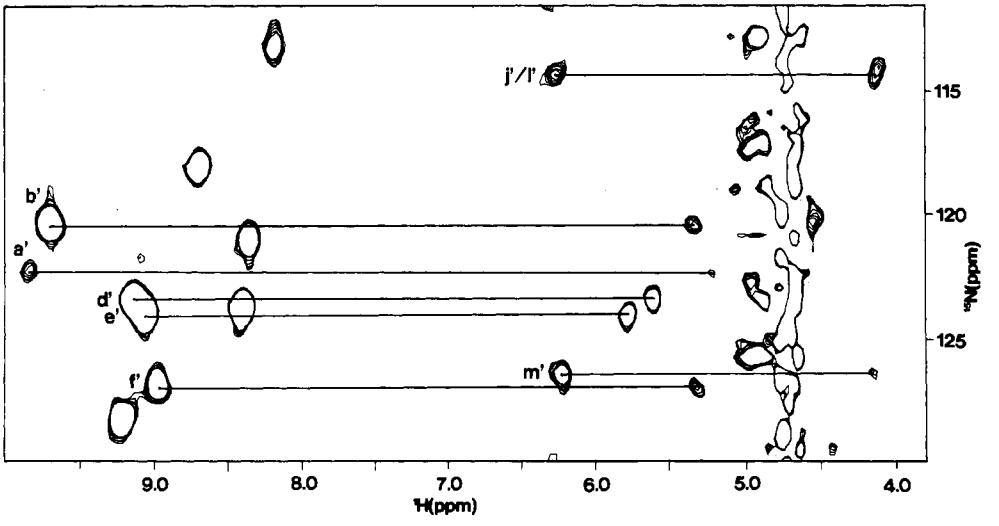

FIGURE 5: Portion of the ^1H–^{15}N HMQC-HOHAHA spectrum of [^{15}N]Fv in H_2O in the presence of DNS-Lys; 30 °C, pH 5.0. Note that resonances a′, b′, d′, e′, and f′ give HOHAHA peaks in the region 5.0–5.8 ppm on the ^1H axis. Details of the spectral measurements are described under Materials and Methods.

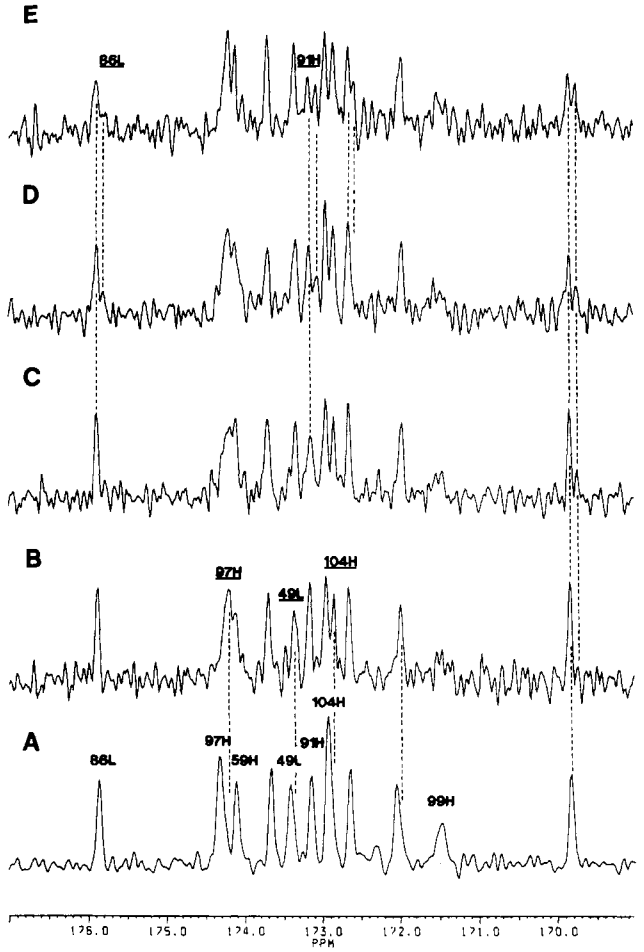

FIGURE 6: 100-MHz ^{13}C NMR spectra of [Y]Fv. After the H_2O solution of the protein was replaced by D_2O by ultrafiltration, spectra were recorded at (A) 0 h (in H_2O), (B) 2.0 h, (C) 10.0 h, (D) 12.5 h, and (E) 19.5 h. In (B), chemical shifts for Tyr-97H, Tyr-104H, and Tyr-49L resonances are different by approximately 0.1 ppm in H_2O and D_2O, indicating that the hydrogen–deuterium exchange was completed within 2 h. Tyr-91H and Tyr-86L peaks were replaced gradually in the time range used in this experiment by a new set of resonances that correspond to the CO-ND peptide. Peaks originating from the CO-ND peptide are identified by using underlined residue numbers. No significant change in chemical shift was observed for Tyr-59H resonance, indicating that hydrogen–deuterium exchange does not occur in the time range used. Concentration and the pH of the sample solution was 0.3 mM and 7.4, respectively. The probe temperature was 30 °C. A total of 8000 transients were accumulated for each spectrum, where 32K data points and a spectral width of 24 000 Hz were used with a delay time of 0.3 s.

Hydrogen–Deuterium Exchange of the NH Protons of Fv Fragment. (i) Use of Carbonyl ^{13}C Resonances. Kainosho and Tsuji (1982) have shown in their ^{13}C NMR study of *Streptomyces* subtilisin inhibitor that (1) when the amide NH proton of a peptide bond is exchanged with deuterium, the carbonyl carbon resonance for this peptide is shifted upfield by approximately 0.1 ppm and (2) this type of isotope effect, which they designated as β-shift, can be used to follow the hydrogen–deuterium exchange. It should be noted that by this method one is observing the exchange through the resonance of the carbonyl carbon that is linked to the NH group under consideration.

^{13}C NMR spectra of [Y]Fv dissolved and incubated in D_2O at pH 7.4 are reproduced in Figure 6, where the spectrum measured in H_2O is also included. Site-specific assignments for seven out of 13 Tyr resonances have been made (Kato et al., 1991b). Figure 6 shows that the hydrogen–deuterium exchange proceeded within 2 h for Tyr-97H, Tyr-104H, and Tyr-49L along with two other Tyr residues. By contrast, even after incubation in D_2O for 20 h, Tyr-59H and two other Tyr residues gave only resonances whose chemical shifts are identical with those observed in H_2O, indicating that the exchange did not occur in this period of time. In the case of Tyr-86L, Tyr-91H, and two other Tyr residues, the exchange rate was between the above two extremes. The rate constants for the amide proton exchange for Tyr-49L, Tyr-97H, and Tyr-104H are larger than 6×10^{-3} min^{-1}. By contrast, in the case of Tyr-59H, hydrogen–deuterium exchange is much slower, with a rate constant smaller than 6×10^{-4} min^{-1}. Tyr-86L and Tyr-91H show an intermediate exchange rate.

Table III: Rate Constants k_m for the Hydrogen–Deuterium Exchange for the Amide Protons of Tyr Residues in [^{15}N]Fv[a]

Tyr residue	location	k_m (min^{-1}) − antigen	k_m (min^{-1}) + antigen
Tyr-58H	CDR2(H)	7.6×10^{-5}	1.4×10^{-4}
Tyr-79H	FR3(H)	0[b]	0
Tyr-90H	FR3(H)	0	0
Tyr-96H	CDR3(H)	f[c]	$<1 \times 10^{-5}$
Tyr-97H	CDR3(H)	f	f
Tyr-99H	CDR3(H)	f	f
Tyr-104H	CDR3(H)	f	0
Tyr-32L	CDR1(L)	1.8×10^{-2}	3.8×10^{-3}
Tyr-36L	FR2(L)	2.1×10^{-3}	5.6×10^{-5}
Tyr-49L	FR2(L)	5.0×10^{-3}	0
Tyr-86L	FR3(L)	1.8×10^{-3}	3.0×10^{-5}

[a] Measured at pH 5.0 and 30 °C. Rate constants for Tyr-59H and Tyr-91H, whose spectral assignments have not yet been established, are not included in here. [b] Exchange did not occur within the time range used, i.e., $k_m < 1 \times 10^{-6}$ min^{-1}. [c] Exchange was too fast to be followed, i.e., $k_m > 1 \times 10^{-1}$ min^{-1}.

Assignments for the Cys resonances observed in the absence and presence of DNS-Lys have already been established (Kato et al., 1991b). The spectral data observed for [C]Fv incubated in D_2O at pH 7.4, 30 °C indicate that hydrogen–deuterium exchange for Cys-22H and Cys-23L was completed within 12 and 24 h, respectively (data not shown). By contrast, the exchange for Cys-98H and Cys-88L was unobservably slow in the time range of this experiment.

The ^{13}C data described above indicate that the exchange of the amide protons of Fv can be followed by observing the carbonyl carbon resonances in D_2O. In the following we will show that measurements of ^1H–^{15}N shift correlation spectra of Fv in D_2O are appropriate in obtaining, with a better time resolution, a more quantitative piece of information about the exchange process.

(ii) Use of ^1H–^{15}N Shift Correlation Spectra of [^{15}N]Fv. Fv fragment labeled with [^{15}N]Tyr was used to follow the hydrogen–deuterium exchange of the amide protons in the absence and presence of DNS-Lys. Figure 7A shows a change in the ^1H–^{15}N shift correlation spectra of Fv, which was incubated in D_2O at pH 5.0 in the absence of DNS-Lys. At different stages of incubation, we were able to observe cross-peaks originating from Tyr residues that had been protected from the hydrogen–deuterium exchange. After incubation for 25 min, five out of the 13 peaks (g, i, j, h, and e) disappeared. Upon a prolonged incubation of 20 h, four additional peaks (b, d, f, and m) lost their intensity. Figure 7B shows the ^1H–^{15}N shift correlation spectra of Fv incubated in D_2O in the presence of DNS-Lys. A significant difference in the rate of hydrogen–deuterium exchange was observed in the absence and presence of DNS-Lys. The rate of hydrogen–deuterium exchange for each of the Tyr resonances has been determined by use of the ^1H cross-section of the ^1H–^{15}N shift correlation spectra, and the results are summarized in Table III.

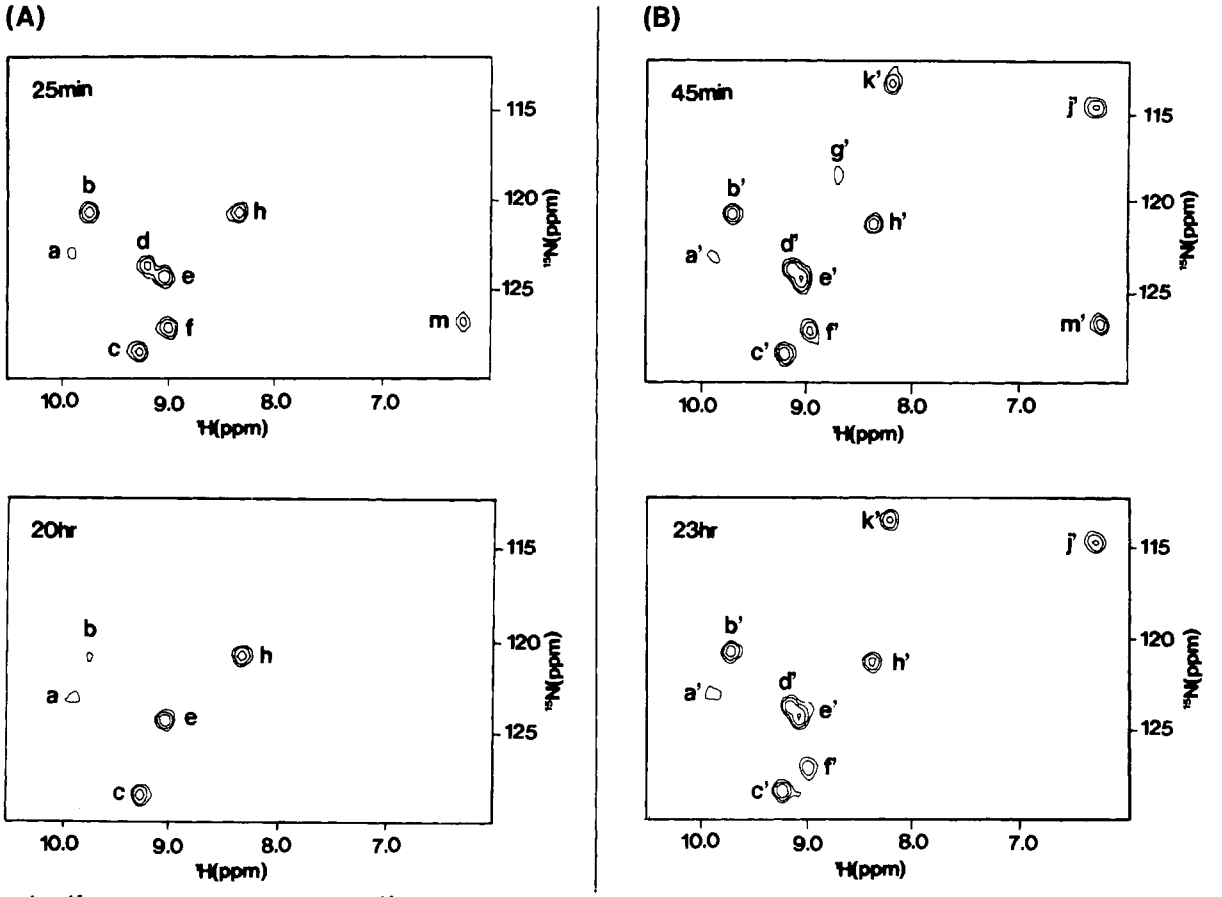

FIGURE 7: $^{1}H-^{15}N$ shift correlation spectra of [^{15}N]Fv in D_2O in the absence (A) and presence (B) of DNS-Lys; 30 °C, pH 5.0. After the protein was dissolved, spectra were recorded at the time indicated in the Figure. Accumulation time for each measurement was 1.0 h. Other spectral conditions are as in Figure 3.

Discussion

Use of Fv Analogues Labeled with ^{2}H, ^{13}C, and ^{15}N for the Study of Antigen Binding. The ^{13}C data obtained so far by using [M]Fv, [W]Fv, [Y]Fv, [C]Fv, and [H]Fv indicate that carbonyl carbon resonances originating from Tyr-97H, His-98H, Tyr-99H, Trp-101H, Tyr-104H, and Trp-105H are under strong influence of DNS-Lys (Kato et al., 1991a,b). It is to be noted that all of these residues belong to the CDR3(H) loop, which possesses the sequence

-Ile^{95}-Tyr-Tyr-His-Tyr-Pro-Trp-Phe-Ala-Tyr-Trp^{105}-

The $^{1}H-^{15}N$ shift correlation spectra of [^{15}N]Fv have shown that Tyr-99H and Tyr-104H resonances are strongly affected by DNS-Lys. The chemical shifts for Tyr-58H and Tyr-79H, which exist in CDR2(H) and FR3(H), respectively, were slightly changed upon antigen binding. However, no other Tyr resonances showed any significant change in chemical shift.

In a previous paper we have concluded on the basis of the NOESY data obtained by use of [^{2}H]Fv that the aromatic rings of two Tyr residues and one of the amide groups are interacting with the dansyl ring of DNS-Lys (Takahashi et al., 1991). In the present work, we have shown by making use of an iodination reaction that one of these two Tyr residues is due to either Tyr-97H or Tyr-99H. This result clearly indicates that the CDR3(H) loop actually makes contact with the aromatic ring of the dansyl group in the Fv–DNS-Lys complex. We therefore conclude that the chemical shift changes observed for the ^{13}C and ^{15}N resonances actually reflect the direct interaction of the CDR3(H) loop with DNS-Lys.

As described above, peaks i and j in the $^{1}H-^{15}N$ shift correlation spectrum of Fv are shifted to a large extent in the presence of DNS-Lys. There exist four Tyr residues in the CDR3(H) loop, i.e., Tyr-96H, Tyr-97H, Tyr-99H, and Tyr-104H. Tyr-99H and Tyr-104H resonances have already been assigned by the double-labeling method. We have already shown that peaks i and j originate from the Tyr-Tyr and Ile-Tyr dipeptides, respectively. We therefore conclude that peaks i and j are due to Tyr-97H and Tyr-96H, respectively (see Table I). This would mean that peaks a, c, and g originate from Tyr-91H (or Tyr-59H), Tyr-90H, and Tyr-59H (or Tyr-91H), respectively. The result of the additional spectral assignments on the basis of the data obtained in the presence of DNS-Lys is also included in Table II.

The HMQC spectrum reproduced in Figure 4 indicates that Tyr-36L, Tyr-49L, Tyr-79H, Tyr-86L, Tyr-59H (or Tyr-91H), and Tyr-58H possess $^{3}J_{HN\alpha}$-coupling constants of 9–11 Hz. This result shows that in these Tyr residues the NH and $C_\alpha H$ bonds are trans to each other. The trans conformation can exist in an extended segment (Wüthrich, 1986). It should be noted that in the HMQC–HOHAHA spectrum shown in Figure 5 Tyr-79H, Tyr-86L, Tyr-36L, and Tyr-49L show the $^{15}N-C_\alpha H$ connectivity. It should be noted that the C_α proton chemical shifts observed for these Tyr residues are lower than that for the H_2O peak. On the basis of these HMQC data we conclude that Tyr-79H, Tyr-36L, Tyr-49L, and Tyr-86L originate from the β-sheet. This is quite consistent with the result of an X-ray crystallographic study of McPC603, which indicates that Tyr-79H, Tyr-36L, Tyr-49L, and Tyr-86L are located in the β-barrel forming the framework of the antigen-binding region (Satow et al., 1986). In the HMQC–HOHAHA spectrum, no cross-peaks were observed for Tyr-59H (or Tyr-91H) and Tyr-58H. Presumably these peaks are buried under the H_2O signal. We suggest that these Tyr

residues exist in an extended segment, which is not involved in the formation of the β-sheet. It should be noted that $^3J_{HN\alpha}$ is undetectably small (≲5 Hz) for Tyr-90H, Tyr-97H, and Tyr-32L. These results suggest that $^3J_{HN\alpha}$-coupling constants measured by HMQC are helpful in discussing the conformation of peptide segments in different parts of the Fv fragment. Selective isotope labeling would play a crucial role in this type of analyses, especially in proteins of the molecular size as studied in the present work.

Hydrogen–Deuterium Exchange of the Amide Protons and the Structure of the Fv Fragment. (i) Cys Residues in the Pin Region of Immunoglobulin Fold. The Fv fragment possesses four Cys residues, two each from the *pin region* of V_H and V_L. It has been shown that there is a large difference in the rate of hydrogen–deuterium exchange for these Cys residues. The exchange for Cys-22H and Cys-23L is much faster than that for Cys-98H and Cys-88L. The X-ray crystallographic data indicate that Cys-98H and Cys-88L are both directed to the interface of the V_H and V_L domains, whereas Cys-22H and Cys-23L face to the open surface of V_H and V_L, respectively (Satow et al., 1986). It has been shown that Cys-98H and Cys-88L are involved in the network of hydrogen bonding. This is consistent with the present observation that these two Cys residues are protected from the hydrogen–deuterium exchange. It should be noted that the exchange for Cys-22H and Cys-23L is much slower than that for residues that are exposed to solvent and do not participate in the formation of hydrogen bonding (Wagner & Wüthrich, 1982). This is especially true in the case of Cys-23L. The crystal data obtained for McPC603 demonstrate that Ala-23H and Arg-24L, which precede Cys-22H and Cys-23L, respectively, both form a hydrogen bond with one of the amino acid residues in the N-terminal segments of the heavy chain and the light chain, respectively. It is therefore possible that the exchange for Cys-22H and Cys-23L reflects the dynamic nature of the hydrogen bonding of Ala-23H and Arg-24L to the N-terminal segments.

(ii) Tyr Residues in the CDR Loops. As summarized in Table III, in the absence of DNS-Lys, the exchange is very fast for five Tyr residues, which include all the four Tyr residues in the CDR3(H) loop, i.e., Tyr-96H, Tyr-97H, Tyr-99H, and Tyr-104H. The ^{13}C data obtained at pH 7.4 for the Tyr carbonyl carbon resonances indicate that in the absence of DNS-Lys the exchange for the NH protons of His-98H and Trp-105H also proceeds very rapidly (see Figure 6). These results indicate that in the absence of DNS-Lys the amide protons of all the Tyr, His, and Trp residues in the CDR3(H) loop do not participate in the formation of hydrogen bonding (Wagner & Wüthrich, 1982).

It is of interest that the hydrogen–deuterium exchange for Tyr-96H and Tyr-104H, two of the four CDR3(H) Tyr residues, became dramatically slow in the presence of DNS-Lys. By contrast, Tyr-97H and Tyr-99H do not show any significant difference in the exchange rate in the absence and presence of DNS-Lys. Tyr-96H and Tyr-104H are located at both ends of the CDR3(H) loop. We conclude that the antigen binding induced a significant degree of conformational change in the CDR3(H) loop, making Tyr-96H and Tyr-104H involved in the network of hydrogen bonding.

It was also possible to follow the exchange for two more Tyr residues that exist in the CDR loop. In the absence of DNS-Lys, the exchange for Tyr-32L, which is located in CDR1(L), was much slower than that described above for the CDR3(H) Tyr residues. The exchange for Tyr-32L became significantly slower in the presence of DNS-Lys. The exchange for Tyr-58H, which exists in the CDR2(H) loop was quite slow. No significant difference in the exchange rate was observed for Tyr-58H in the absence and presence of DNS-Lys.

(iii) Tyr Residues in the Framework Region of V_H and V_L. Table III indicates that the exchange is undetectably slow for Tyr-79H, Tyr-90H, and Tyr-91H. All of these residues, which are located in FR3(H), presumably participate in the formation of hydrogen bonding. Addition of DNS-Lys did not affect at all the rate of exchange for these residues. By contrast, Tyr-36L, Tyr-49L, and Tyr-86L, all of which exist in FR2(L), behave in quite a different way in the hydrogen–deuterium exchange. The rate of exchange for all of these Tyr residues observed in the absence of DNS-Lys was of the order of 10^{-3} min^{-1}. The exchange for these Tyr residues became slow by 2 orders of magnitude in the presence of DNS-Lys (see Table III). It should particularly be noted that the antigen binding reduced the exchange rate for Tyr-49L to the level that is observed in the case of the heavy chain Tyr resonances in the framework region (vide supra).

We have shown above that (1) in the absence of DNS-Lys the exchange for Tyr residues in the FR of the light chain is much faster than that in the FR of the heavy chain but (2) the exchange rate for the heavy and light chains becomes comparable in the presence of DNS-Lys. The X-ray crystallographic data show that all the Tyr residues of V_L are located on the interface between the V_H and V_L domains. We therefore suggest that in the presence of DNS-Lys these two domains form a more extensive network of hydrogen bonding, making a closer contact with each other.

The results obtained here are of interest in that, upon binding of a small hapten like DNS-Lys, a significant change in the rate of hydrogen–deuterium exchange is induced in both ends of the CDR3(H) loop and the effect of the antigen binding is extended over a wider range in the two-domain Fv fragment including the V_L domain. The results reported here indicate that the exchange of the amide protons is much more sensitive than the chemical shifts in following the subtle change in the mode of domain–domain interactions (Englander & Kallenbach, 1984). Use of a DEALS method (Kainosho et al., 1987) would be helpful in following faster exchange of the amide protons. This line of approach is now further being pursued with use of three-domain Fab* and four-domain Fab fragments that have also been derived from the switch variant IgG2a antibody.

Concluding Remarks. One of most intriguing questions about the antigen–antibody interactions has been whether any conformational change occurs in association with antigen binding (Davies et al., 1990). X-ray diffraction is potentially the most direct method in answering this question. Some of the problems that are inherent in the interpretation of the crystal structure of proteins include intermolecular interactions in the crystal and the presence of a large amount of inorganic salts.

NMR is another possible method for the discussion of antigen–antibody interactions at atomic resolution. An important aspect of NMR is that it can give information about dynamic structures of proteins in solution. Thus, NMR can in principle be a direct method in discussing possible changes in conformation of the antibody in solution in the absence and presence of antigen. One of the problems inherent in applying NMR to proteins is to separately observe and assign resonances that can be used as spectroscopic probes. Obviously, this is in general difficult in the case of antibodies and their fragments in view of the large number of amino acid residues that gives

similar chemical shifts. Therefore, appropriate methods should be explored in order to extract relevant information as much and as selective as possible.

In the present study, we have shown that multinuclear NMR analyses of the Fv fragment, which is half in size of the Fab fragment, make it possible to collect information that is necessary to discuss the static and dynamic structure of the antigen-binding site in the absence and presence of the antigen. On the basis of the results obtained in this work, we are currently developing NMR analyses of the structure of a variety of functional fragments derived from the switch variant antibodies. Bhat et al. (1990) have recently reported that antigen binding induces small rearrangements in the structures of Fv and Fab fragments of anti-lysozyme antibody. This result is of particular interest in view of the conformational change observed in the present work through the rate of hydrogen–deuterium exchange. Combination of X-ray crystallographic analyses and NMR would certainly become of increasing importance in discussing the static and dynamic structure of antibodies.

ACKNOWLEDGMENTS

We thank Professor L. A. Herzenberg, Stanford University, and Dr. V. T. Oi, Becton Dickinson Immunocytometry Systems, for generously providing us with the mouse hybridoma cell line 1B10.7 and also for making the amino acid sequence data of the variable regions available to us prior to publication. We also thank Dr. N. Sugita, Kureha Chemical Industry Co., Ltd., for the gift of [1-^{13}C]cystine. We are grateful to Professor H. Yamada and Dr. T. Nagasawa, Kyoto University, for letting us use their facility and for their help in the preparation of β-tyrosinase and to Professor R. J. Poljak for making the preprint of his work available to us prior to publication. We are grateful to Dr. M. Oyabu, Shimadzu Corporation, for the use of the GE Omega 500 spectrometer.

Registry No. DNS-Lys, 1101-84-4.

REFERENCES

Bax, A., Griffey, R. H., & Howkins, B. L. (1983) *J. Am. Chem. Soc. 105*, 7188–7190.

Bhat, T. N., Bentley, G. A., Fischmann, T. O., Boulot, G., & Poljak, R. J. (1990) *Nature 347*, 483–485.

Bodenhausen, G., & Ruben, D. J. (1980) *Chem. Phys. Lett. 69*, 185–189.

Boulot, G., Eisele, J.-L., Bentley, G. A., Bhat, T. N., Ward, E. S., Winter, G., & Poljak, R. J. (1990) *J. Mol. Biol. 213*, 617–619.

Dangl, J. L. (1986) Ph.D. Thesis, Stanford University.

Dangl, J. L., Parks, D. R., Oi, V. T., & Herzenberg, L. A. (1982) *Cytometry 2*, 395–401.

Davies, D. R., Padlan, E. A., & Sheriff, S. (1990) *Annu. Rev. Biochem. 59*, 439–473.

Englander, W., & Kallenbach, N. R. (1984) *Q. Rev. Biophys. 16*, 521–655.

Gronenborn, A. M., Bax, A., Wingfield, P. T., & Clore, G. M. (1989) *FEBS Lett. 243*, 93–98.

Hochman, J., Inbar, D., & Givol, D. (1973) *Biochemistry 12*, 1130–1135.

Huston, J. S., Levinson, D., Mudgett-Hunter, M., Tai, M.-S., Novotny, J., Margolies, M. N., Ridge, R. J., Bruccoleri, R. E., Haber, E., Crea, R., & Oppermann, H. (1988) *Proc. Natl. Acad. Sci. U.S.A. 85*, 5879–5883.

Igarashi, T., Sato, M., Katsube, Y., Takio, K., Tanaka, T., Nakanishi, M., & Arata, Y. (1990) *Biochemistry 29*, 5727–5733.

Inbar, D., Hochman, J., & Givol, D. (1972) *Proc. Natl. Acad. Sci. U.S.A. 69*, 2659–2662.

Kabat, E. A., Wu, T. T., Reid-Miller, M., Perry, H. M., & Gottesman, K. S. (1987) *Sequences of Proteins of Immunological Interest*, 4th ed., U.S. Department of Health and Human Services, National Institutes of Health, Washington, DC.

Kainosho, M., & Tsuji, T. (1982) *Biochemistry 21*, 6273–6279.

Kainosho, M., Nagao, H., & Tsuji, T. (1987) *Biochemistry 26*, 1068–1075.

Kato, K., Matsunaga, C., Nishimura, Y., Waelchli, M., Kainosho, M., & Arata, Y. (1989a) *J. Biochem. (Tokyo) 105*, 867–869.

Kato, K., Nishimura, Y., Waelchli, M., & Arata, Y. (1989b) *J. Biochem. (Tokyo) 106*, 361–364.

Kato, K., Matsunaga, C., Igarashi, T., Kim, H., Odaka, A., Shimada, I., & Arata, Y. (1991a) *Biochemistry 30*, 270–278.

Kato, K., Matsunaga, C., Odaka, A., Yamato, S., Takaha, W., Shimada, I., & Arata, Y. (1991b) *Biochemistry* (preceding paper in this issue).

Kay, L. E., & Bax, A. (1990) *J. Magn. Reson. 86*, 110–126.

Lesk, A. M., & Chothia, C. (1982) *J. Mol. Biol. 160*, 325–342.

Marion, D., & Wüthrich, K. (1983) *Biochem. Biophys. Res. Commun. 113*, 967–974.

Markley, J. L. (1989) *Methods Enzymol. 176*, 12–64.

Markley, J. L., Putter, I., & Jardetzky, O. (1968) *Science 161*, 1249–1251.

Mueller, L. (1979) *J. Am. Chem. Soc. 101*, 4481–4484.

Nagasawa, T., Utagawa, T., Goto, J., Kim, C., Tani, Y., Kumagai, H., & Yamada, H. (1981) *Eur. J. Biochem. 117*, 33–40.

Norwood, T. J., Boyd, J., & Campbell, I. D. (1989) *FEBS Lett. 255*, 369–371.

Redfield, A. G. (1983) *Chem. Phys. Lett. 96*, 537–540.

Riechmann, L., Foote, J., & Winter, G. (1988) *J. Mol. Biol. 203*, 825–828.

Satow, Y., Cohen, G. H., Padlan, E. A., & Davies, D. R. (1986) *J. Mol. Biol. 190*, 593–604.

Sharon, J., & Givol, D. (1976) *Biochemistry 15*, 1591–1594.

Skerra, A., & Plückthun, A. (1988) *Science 240*, 1038–1041.

States, D. J., Hakerkorn, R. A., & Ruben, D. J. (1982) *J. Magn. Reson. 48*, 286–292.

Takahashi, H., Igarashi, T., Shimada, I., & Arata, Y. (1991) *Biochemistry 30*, 2840–2847.

Wagner, G., & Wüthrich, K. (1982) *J. Mol. Biol. 160*, 343–361.

Ward, E. S., Gussow, D., Griffiths, A. D., Jones, P. T., & Winter, G. (1989) *Nature 341*, 544–546.

Wright, P. E., Dyson, H. J., Lerner, R. A., Riechmann, L., & Tsang, P. (1990) *Biochem. Pharmacology 40*, 83–88.

Wüthrich, K. (1986) in *NMR of Proteins and Nucleic Acids*, Wiley, New York.